The Mechanism of Phosphorylation of Natural Nucleosides and Anti-HIV Analogues by Nucleoside Diphosphate Kinase Is Independent of Their Sugar Substituents

Michael C. Hutter and Volkhard Helms*[a]

The reaction mechanism of the phosphoryl transfer catalyzed by dinucleoside diphosphate kinase from Dictyostelium discoideum *is investigated by semiempirical AM1 molecular orbital computation of an active site model system on the basis of various X-ray crystallographic structures. The computational results suggest that the phosphoryl transfer from adenosine triphosphate to the His122 residue is accompanied by the simultaneous shift of a proton from the histidine residue to one of the oxygen atoms of the γ phosphate group. This involves a doubly protonated His122 residue whilst this residue is neutral in its ternary complex with ADP and the transition state analogue AlF_3. The proposed mechanism is thus analogous to that of phosphoryl transfer by cyclic adenosine monophosphate dependent protein kinase and uridine/cytidine monophosphate kinase as found in our earlier work and clarifies the role of the ribose 3′-OH group. Furthermore, the energetics of phosphoryl transfer onto other nucleoside analogues such as 3′-azido-3′-deoxythymidine-diphosphate and 2′,3′-dideoxy-2′,3′-didehydrothymidine-diphosphate are investigated. The calculated reaction barriers for the phosphorylation of the diphosphates by the enzyme are all within a range of 13.1 kJ mol^{-1}, which suggests that variations in the activation energies alone cannot account for the experimentally observed differences in enzymatic activity. Consequences for the design of new anti-HIV nucleoside analogues are discussed.*

KEYWORDS:

antiviral agents · molecular modeling · reaction mechanisms · semiempirical calculations · transition state analogues

Introduction

Kinases are enzymes that mediate the formal transfer of a PO_3 (phosphoryl) group from the triphosphate nucleoside adenosine triphosphate (ATP) to an acceptor molecule. The possible acceptor groups are diverse since phosphorylation is used in biological processes like energy and signal transduction, activation of metabolites, cell growth, and cellular regulation.[1–3] The latter two processes require nucleoside triphosphates other than ATP that are synthesized from the corresponding diphosphates by nucleoside diphosphate kinase (NDPK). For example, 2′-deoxythymidine diphosphate (dTDP) is converted into 2′-deoxythymidine triphosphate (dTTP), which is required for DNA synthesis. This makes NDPK a key enzyme to be considered in the development of antiviral treatments because the diphosphates of agents such as 3′-azido-3′-deoxythymidine (AZT), which lacks the 3′-OH group necessary for the elongation of the DNA backbone, also have to be phosphorylated by NDPK. Unfortunately, AZT-diphosphate (AZT-DP) is only a poor substrate for NDPK as both its binding affinity[4, 5] and the phosphorylation capacity of human NDPK B[6] are several orders of magnitude lower than for natural nucleoside diphosphates such as dTDP.

It was suggested that the 3′-OH group of the nucleosides also plays a role in the catalytic phosphorylation mechanism of NDPK[7] because this OH group forms a hydrogen bond to, or may even donate its proton to the γ phosphate group of the nucleoside. If this interaction is of importance, it explains the low phosphorylation rate of dideoxynucleosides like AZT-DP, which cannot be stabilized by such an interaction. On the other hand, the dissociation constants of the natural substrate dTDP and 2′,3′-dideoxy-2′,3′-didehydrothymidine diphosphate (D4T-DP) for binding with a mutant of NDPK that is enzymatically inactive are quite similar to one another. Furthermore, the phosphorylation rate of D4T-DP is much higher than that of AZT-DP.[4] The general picture that emerges is that variations in the rate of phosphorylation of the various nucleosides are mostly determined by differences in their binding affinities. It is currently unclear what kind of stabilization can be ascribed to the 2′- and 3′-OH groups and whether there exist significant differences in the activation barrier for phosphoryl transfer as was suggested to be the case for poor substrates.[7] The issue of activation

[a] *Dr. V. Helms, Dr. M. C. Hutter*
Theoretical Biophysics
Max-Planck-Institute of Biophysics
Kennedyallee 70, 60596 Frankfurt (Germany)
Fax: (+49) 69-6303-251
E-mail: Volkhard.Helms@mpibp-frankfurt.mpg.de

Supporting information for this article is available on the WWW under http://www.chembiochem.com or from the author.

barrier differences can only be addressed by separation of the phosphoryl transfer reaction from the binding step, which can be done by quantum chemical calculations.

The sequences and the three-dimensional structures of nucleoside diphosphate kinases from various organisms are highly conserved, particularly in the active site region.[8–10] NDPK from the lower eukaryote *Dictyostelium discoideum* (Dd-NDPK) considered here shows similar kinetic parameters to human nucleoside diphosphate kinases.[11] This makes Dd-NDPK a suitable model for eukaryotic NDPK.

In contrast to most other kinases, which directly transfer the phosphoryl group from ATP to the acceptor, catalysis by NDPK involves the formation of a covalent phosphohistidine in the active center of the enzyme (E) [Eq. (1); $\sim$ indicates reversibly bonded species, in this case the enzyme and a PO_3 group].[7] After the release of ADP, a different dinucleoside, XDP, can bind at the same position to be subsequently phosphorylated [Eq. (2)].[12–14]

$$E + MgATP \leftrightarrow E \sim P + MgADP \quad (1)$$

$$E \sim P + MgXDP \leftrightarrow E + MgXTP \quad (2)$$

Although the phosphorylation of histidine is fully reversible,[15] the transient phosphorylated enzyme without ADP and magnesium (1NSP) is stable for a few hours at low temperature and could be crystallized.[14] Numerous other X-ray crystallographic structures of Dd-NDPK[9]have been reported and include the holoenzyme (1NPK)[16] and the ternary complex of the enzyme with ADP·Mg and the transition state analogue AlF_3 (1KDN).[17] These structures outline the catalytic pathway.[7] This "ping-pong mechanism" proceeds through an intermediate high-energy phosphohistidine[14] and this state can be regarded as the primary product of the phosphoryl transfer from ATP, which may have a similar mechanism to that seen in other kinases.[1]

Enzymatic phosphoryl transfer is commonly discussed on the basis of structural and electronic properties in terms of the two extremes "associative" and "dissociative".[18] A fully dissociative mechanism requires a certain distance between ATP and the accepting group so that the γ phosphate group can be completely removed from ATP to form a monoanionic metaphosphate in the transition state. Conversely, a fully associative mechanism involves a strongly negatively charged metaphosphate with a penta-coordinated phosphorus atom whose apical ligands are within the range of covalent single bonds (around 1.7 Å). Conclusive information about the actual charge on the metaphosphate can, however, only be derived from quantum chemical calculations.

Crystallographic studies of NDPK and uridine/cytidine monophosphate kinase (UMP/CMP kinase) in the presence of ADP have been reported that also incorporate the so-called transition state analogues aluminum fluoride and beryllium fluoride, respectively.[17, 19] Although AlF_3 mimics the planar shape of the metaphosphate (PO_3) in the supposed transition state, the total charge of the reactants is different: ATP·Mg has a charge of -2 while Mg·ADP·AlF_3 has a net charge of -1. Furthermore it was suggested in a recent quantum chemical study that the presence of aluminum trifluoride alters the protonation state of the phosphoryl-accepting mononucleoside in UMP/CMP kinase.[20] It was found that the α phosphate group of UMP or CMP should be protonated to enable phosphoryl transfer, while the mononucleoside is likely to be unprotonated in the presence of ADP·AlF_3. Such quantum chemical methods are ideal for investigation of reaction mechanisms and determination of the structures of transition states as these states are well-defined saddle points along a reaction coordinate which connects reactants and products. It is therefore relatively straightforward to study the influence on the reaction mechanism of subtle substitutions in the substrate once the mechanism itself has been established, for example, effects upon the activation barrier can be determined. For UMP/CMP kinase and cyclic adenosine monophosphate dependent protein kinase (cAPK) the computed phosphoryl transfer reactions revealed the participation of a proton that is simultaneously shifted to one of the oxygen atoms of the PO_3 group as the phosphoryl is transferred. This put the reaction mechanism of kinases in a new light.[20–22]

The investigation of the phosphoryl transfer mechanism in NDPK with quantum chemical methods in this work will help improve understanding of the substrate properties of nucleoside analogues and is moreover another step towards a common enzymatic reaction mechanism for all kinases.

Results

The structures of all investigated nucleosides are given in Scheme 1 for clarity. We first consider one of the native ping-pong reactions of NDPK, the phosphoryl group shuttle between ATP and dTDP, in order to establish a firm basis for the analysis of the AZT-DP reaction.

Adenosine triphosphate/adenosine diphosphate and AlF_3

The molecular system shown in Scheme 2 (see the Methods Section for details) corresponds to the reactant state in which ATP and magnesium are bound to the enzyme. It has a net neutral charge as the His122 residue is expected to be doubly protonated in the presence of ATP. If both the His122 residue and ATP are unprotonated the model that results is a structure in which the nonplanar γ PO_3 group is covalently bound neither to the δ nitrogen of the His122 residue nor to the bridging oxygen of ADP. This geometry cannot be regarded as a transition state or reactant geometry. Interestingly, the same geometry is also obtained when the optimization is started from the supposed product state, which is more than 146 kJ mol^{-1} higher in energy than the reactant state and comprises phosphorylated histidine (His-PO_3) and ADP. Therefore, neither the reactant nor the product state yields a stable geometry when both the His122 residue and ATP are treated as unprotonated. These results are, however, not surprising from an electrostatic point of view as the interaction between an unprotonated δ nitrogen and a negatively charged γ PO_3 group is unfavorable. When the γ phosphate group is replaced by the uncharged AlF_3 molecule, the geometry optimization yields a structure that resembles a transition state in which the aluminum atom is apically

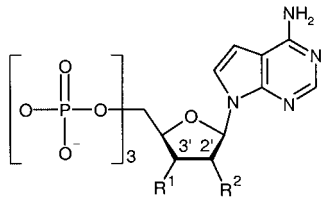

a: adenosine-β-D-ribose triphosphate

ATP R^1 = OH, R^2 = OH

2'-*d*ATP R^1 = OH, R^2 = H

3'-*d*ATP R^1 = H, R^2 = OH

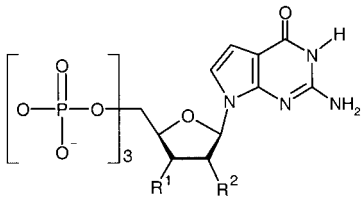

b: guanosine-β-D-ribose triphosphate

GTP R^1 = OH, R^2 = OH

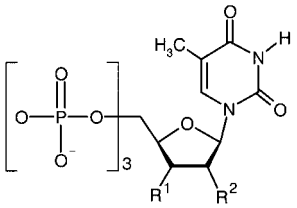

c: thymidine-β-D-ribose triphosphate

*d*TTP R^1 = OH, R^2 = H

TTP R^1 = OH, R^2 = OH

AZT-TP R^1 = N_3, R^2 = H

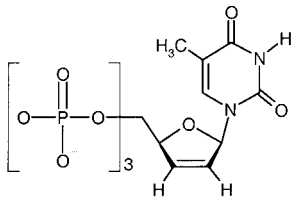

d: D4T-triphosphate

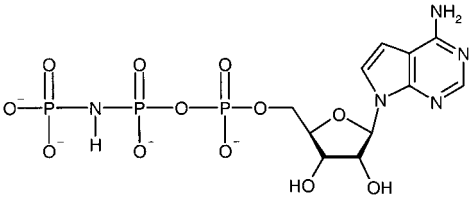

e: adenosine-5'-[β-γ-imido]-triphosphate (AMP-PNP)

Scheme 1. *The structures of the investigated nucleosides.*

coordinated by N_δ and by the bridging oxygen of ADP. This result is in agreement with the crystal structure of the system in which AlF_3 and ADP · Mg are complexed with the enzyme.[17] Conversely, when doubly protonated histidine with ATP is considered, calculations yield the reactant structure shown in Scheme 2. The proton added at the His-N_δ atom points towards the γ phosphate oxygen atom (O1C), which also coordinates the magnesium ion. The plane of the histidine ring is turned slightly towards the Tyr56 residue compared to its position in the crystal structure that contains AlF_3 (1KDN) but is in the same plane as the Tyr56 residue in the crystal structure that contains the phosphorylated histidine (1NSP). The side chains of the Lys16 and Tyr56 residues, which are involved in hydrogen bonding to the γ PO_3 group do not show any significant movement upon the exchange of AlF_3. Only the solvent-exposed adenine moiety in ATP shows noteworthy deviations in position, while the positions of the phosphate groups are closely retained. These structural movements are caused by the omission of the outer parts of the protein from our computational model but are unlikely to affect the computed energies since the active site is preserved.

We found two conceivable product structures for the phosphoryl transfer onto the His122 residue in which the N_δ proton is shifted to the closest oxygen (O1C) atom of the γ phosphate group. The first product is 66.9 kJ mol^{-1} higher in energy than the reactant and has the O1C oxygen atom still bound to the magnesium ion while the remaining ADP stays almost in place. The plane of the histidine ring is slightly turned upwards and the phenyl ring of the Tyr56 residue is rotated outwards by about 20° but still forms a hydrogen bond with the γ phosphate O3C atom. This situation is similar to that found in the X-ray structure which corresponds to the product (1NSP). This structure can be regarded as the product of a minimum motion transfer of atoms. In the second geometry, which is only 23.4 kJ mol^{-1} higher in energy than the reactant, the α and β phosphate groups of ADP are moved towards the histidine and the adenosine moiety is translated by about 0.7 Å. In this case the shifted proton is stabilized by a hydrogen bond with a water molecule (HOH612 in 1KDN or HOH228 in 1NSP, respectively). As the transferred γ PO_3 group is rotated, the magnesium ion is now ligated by a different oxygen atom (O2C). The formation of this

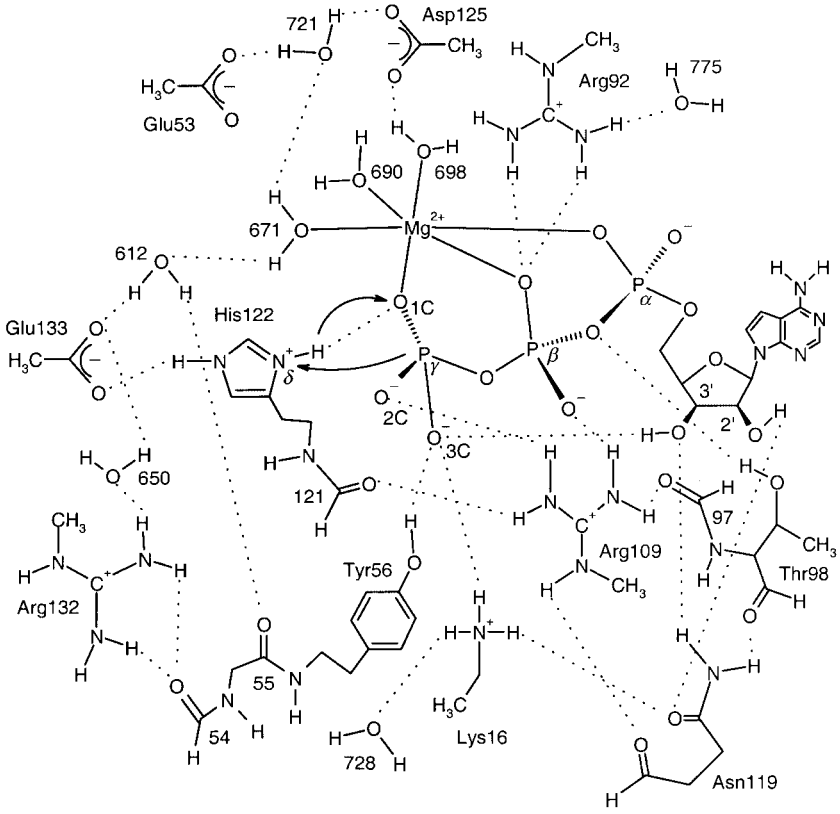

Scheme 2. *The quantum mechanical model system used to study the phosphoryl transfer. A bound ATP molecule and the considered residues in the active site are shown. The model is derived from the 1KDN crystal structure of NDPK complexed with ADP and AlF_3 and with ADP · AlF_3 replaced by ATP.*

product geometry, however, requires a transient change of the coordination sphere of the magnesium ion, which is an energetically unfavorable process (see below).

To characterize the activation barrier for the transfer of the phosphoryl group onto the His122 residue in the first product geometry, a reaction path calculation was performed. In this reaction path, the P_γ atom is moved towards the N_δ atom of the His122 residue while the proton is simultaneously shifted from the N_δ atom to the O1C oxygen atom of the γ phosphate group as indicated by the arrows in Scheme 2. We found an activation barrier of 148.4 kJ mol^{-1} to reach the transition state. Conversely the reaction barrier for the reverse reaction, the transfer of a phosphoryl group from phosphohistidine to ADP, is 81.5 kJ mol^{-1} (see Table 1). The proton position in the transition state is similar to that obtained previously for cAPK and UMP/CMP kinase.[20, 21] The proton sits inbetween the phosphorus-accepting atom (N_δ of His122) and the oxygen of the transferred γ PO_3 group (O1C). The P_γ atom is still bound to the oxygen atom of the β phosphate group (1.692 Å). The γ phosphate group is not planar and the P_γ atom is within 2.413 Å of N_δ (3.474 Å in the reactant). Analysis of the transition state by calculation of its harmonic vibrations gave a single imaginary frequency of -1003 cm^{-1} associated with the movement of the shifted proton after a deformational vibration of the N_δ—H bond. This type of vibration was also found in the transition states of all other nucleoside systems investigated. Although the respective frequencies range from -971 cm^{-1} (3′-dATP) to -1504 cm^{-1} (AZT-TP), the geometries of the involved molecular fragments are very similar. The mechanism derived from these results is shown on the left of Scheme 3. We computed the activation barrier that must be overcome to reach the alternative product (see above) to be 54 kJ mol^{-1} higher than that for the reaction path described above as a result of the change in the coordination sphere of the magnesium ion. This alternative reaction is therefore not likely to happen.

Table 1. *Computed energies for the phosphoryl transfer from triphosphate nucleosides onto NDPK (XTP →E ∼ P), and from the phosphorylated enzyme onto diphosphate nucleosides (E ∼ P →XTP).*[a]

Nucleoside system	Reaction barrier $\Delta H^{\neq}$ (XTP →E ∼ P)	Reaction enthalpy ΔH_{react}	Reaction barrier $\Delta H^{\neq}$ (E ∼ P →XTP)
ATP	148.4	+66.9	81.5
2′-dATP	152.2	+73.6	78.6
3′-dATP	152.6	+83.4	69.2
GTP	150.5	+69.2	81.3
TTP	140.9	+66.2	74.7
dTTP	151.3	+71.5	79.8
D4T-TP	157.2	+79.3	77.9
AZT-TP	163.0	+80.7	82.3
AMP-PNP	185.6	−64.4	-

[a] The associated energy profile is shown in Figure 1. All energies are given in kJ mol^{-1}. The system that contains the triphosphate (E:MgXTP) is taken as the reference point (±0.0) in each nucleoside system.

Energetic minimization of the molecular system that contains ADP and the transition state analogue AlF_3, which is the transition state model usually used, yields a planar aluminum trifluoride molecule in accordance with the crystallographic structure. The aluminum atom is apically coordinated by the N_δ atom of the (unprotonated) His122 residue (2.420 Å) and the oxygen atom of the β phosphate group (2.336 Å). These computed distances are in good agreement with the X-ray data (2.427 and 2.413 Å, respectively).

2′-Deoxythymidine triphosphate

dTDP is a typical natural substrate for phosphorylation by NDPK. This involves the reverse of the reaction discussed above, that is,

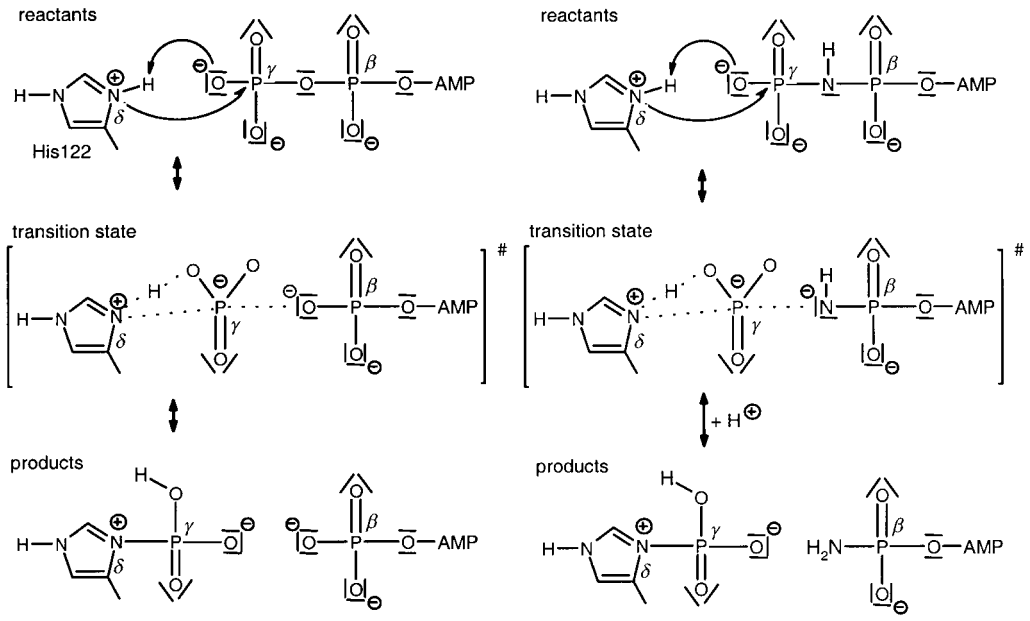

Scheme 3. *The concerted phosphoryl transfer mechanism as suggested from quantum chemical calculations involves the synchronous shift of a proton from the protonated His122 residue (left). Processing of adenosine-5′-[β,γ-imido]-triphosphate (AMP-PNP) produces an intermediate imido anion that can adopt a proton from a nearby group, for example from the 3′-OH group of the ribose moiety (right).*

transfer of a PO_3 group from the phosphorylated His122 residue to the β phosphate group of the nucleoside diphosphate. The optimized geometry of the reactant is nearly identical to that for ADP. As a result of the missing hydrogen bond between the 2′-deoxyribose and the side chain of the Asn119 residue, the latter rotates outwards by around 35° and the hydrogen bond to the carbonyl oxygen atom of the Thr98 residue is thereby shortened by about 0.1 Å. An activation energy of 151.3 kJ mol^{-1} was obtained for the phosphorylation of the His122 residue by calculation of the reaction path. This result corresponds to a reaction barrier of 79.8 kJ mol^{-1} for the phosphoryl transfer onto dTDP. Both values are very similar to those of the ATP/ADP system.

3′-Azido-3′-deoxythymidine

The in vivo phosphorylation of AZT diphosphate by NDPK is inefficient.[6] The 2′-deoxyribose ring of AZT has the 3′-OH group substituted by an N_3 group, which causes several hydrogen bonds to be broken compared to the situation for the natural analogue dTDP. As shown in Scheme 2, the 3′-OH group of ATP donates a hydrogen bond to the O3C oxygen atom of γ phosphate and accepts one from the amino group in the side chain of the Asn119 residue. The carbonyl oxygen atom of the Asn119 side chain accepts hydrogen bonds from the Lys16 residue and 2′-OH group. Binding of deoxyribose nucleosides that lack the 2′-OH group is therefore unfavorable. In addition, the presence of the N_3 group on AZT phosphate is electrostatically and sterically unfavorable in the active site.

The reported X-ray structure of NPDK complexed with AZT-DP (1LWX)[23] is that of a mutant in which the Asn119 residue is replaced by alanine. It shows a significant structural deviation in the active site compared to the crystal structure of NDPK complexed with thymidine diphosphate but the rest of the protein structure is unaltered. The side chain of the Lys16 residue in the 1LWX structure is turned outwards, which was ascribed to the steric effect of the 3′-azido group. In our computed geometries of the product and reactant states of the AZT nucleosides bound to wild-type NDPK we found no such movement of the side chain of the Lys16 residue but an outward turn of the Asn119 residue through about 50° was seen as a result of the presence of the N_3 group. The hydrogen bond between the Lys16 and Asn119 residues is conserved.

The complex of the phosphorylated histidine and AZT-DP (His122-PO_3H · AZT-DP) is 80.7 kJ mol^{-1} higher in energy than the complex that contains the triphosphate of AZT (His122-H · AZT-TP). The activation energy for the transfer of a phosphoryl group onto AZT-DP is 82.3 kJ mol^{-1} (compared with 81.5 kJ mol^{-1} for the corresponding phosphoryl transfer to ADP). The reaction path calculation yields an activation barrier for the phosphorylation of histidine of 163.0 kJ mol^{-1} (148.4 kJ mol^{-1} with ATP).

2′,3′-Dideoxy-2′,3′-didehydrothymidine triphosphate (D4T-TP)

To circumvent the disadvantages involved with the azido group in AZT, a double bond between the C2′ and C3′ atoms of the ribose moiety was introduced into the clinically relevant nucleoside analogue D4T. The crystal structure of the enzymatically inactive H122G mutant of NDPK complexed with D4T-TP (1F3F)[24] indeed reveals that the conformation of the Lys16 residue is preserved while the ribose moiety is turned slightly inwards to allow hydrogen-bond-like interactions between 3′-CH group and the O3C oxygen atom of the γ phosphate group as well as the P_β—P_γ bridging oxygen. The side chain of the Asn119 residue shows no noticeable changes compared to the 1KDN crystal structure, which contains ADP · AlF_3.[17] Our computed geometries for D4T-TP and D4T-DP in the active site model agree with all of these structural findings. We found a distance of 2.007 Å between the 3′-CH group and the O3C oxygen atom in the product (D4T-DP), which is 79.3 kJ mol^{-1} higher in energy than His122-H · D4T-TP. A reaction barrier of 77.9 kJ mol^{-1} was calculated for the transfer of a phosphoryl group onto D4T-DP.

2′-Deoxyadenosine triphosphate (2′-dATP)

Like dTDP, 2′-deoxyadenosine diphosphate lacks the 2′-OH group on its ribose moiety and shows the same structural movement of the Asn119 side chain. There is no difference between the reaction barrier for the reversible phosphoryl transfer for dADP/dATP and for that ADP/ATP in either direction within the error limit of the underlying method.

3′-Deoxyadenosine triphosphate

In contrast to D4T, 3′-dADP cannot form favorable interactions between the 3′-CH group and the phosphorylated histidine. Interestingly, E ~ Mg complexed with 3′-dADP is 83.4 kJ mol^{-1} higher in energy than the complex with the triphosphate which is the largest difference among the investigated nucleosides. This destabilization is also reflected by the low reaction barrier for the phosphoryl transfer to the diphosphate (+ 69.2 kJ mol^{-1}), while the activation barrier for the forward reaction is similar to that for 2′-dATP.

2′-Hydroxythymidine triphosphate (TTP)

In contrast to the naturally occurring dTDP, thymidine-diphosphate (TDP) is a hypothetical substrate which possesses a 2′-OH group and is thus analogous to ADP. Among the investigated nucleoside analogues it shows the lowest activation barriers for the phosphoryl transfer in both directions (140.9 for phosphorylation of TDP and 74.7 kJ mol^{-1} for the backward reaction), although no apparent structural differences compared to the computed geometries of the transition states for ATP and dTTP are noticeable. Interestingly, the calculated imaginary frequency (− 973 cm^{-1}) is the lowest among the investigated pyrimidine-type nucleosides.

As the reaction barrier for the phosphoryl transfer from TTP onto His122 is somewhat lower (6.8 kJ mol^{-1}) than for the corresponding reaction involving ATP, the (hypothetical) TTP could compete successfully with ATP in phosphorylation of NDPK and would thus leave a much lower level of TTP available for further biosynthetic use than is the case for the naturally occurring dTTP.

Adenosine-5′-[β,γ-imido]-triphosphate (AMP-PNP)

Substitution of the oxygen atom that links the β and γ phosphorus atoms by an NH group results in an ATP analogue that is still slowly processed by NDPK but is a strong inhibitor of other phosphotransferases.[7, 17] Cleavage of the γ PO_3 group as required for phosphorylation of the His122 residue, however, results in a chemically unstable HN—$P(O_2)$O—R (R = the nucleoside) fragment that can easily accept a proton from a nearby group, presumably the Lys16 residue or the 3′-OH group of the ribose moiety as was suggested for the mechanism of phosphoryl transfer in NDPK.[6] The 3′-hydroxylate anion that results from proton donation by the 3′-OH group would be able to pick up another proton from solution upon release from the binding pocket (see right-hand side of Scheme 3). During the reaction path calculation we actually observed the transfer of the proton from the 3′-OH group to the imido nitrogen which, however, occurs alongside the shift of the N_δ proton to O1C and requires an activation energy of 185.6 kJ mol^{-1}. The transition state for this concerted reaction shows an imaginary frequency of -1776 cm^{-1}. The resulting product, which contains the unprotonated 3′-hydroxy group, is 64.4 kJ mol^{-1} lower in energy than the reactants. This exothermic step therefore implies a reaction barrier of 250 kJ mol^{-1} for the reverse reaction, which is thus very unlikely.

Other kinases[1] do not bind ATP in a geometry in which the ribose 3′-hydroxy hydrogen atom points in the direction of the γ phosphate group. This fact may explain the inhibitory property of adenosine-5′-[β,γ-imido]-triphosphate.

Discussion

It has been suggested that within the pH range in which NDPK is active (pH 7 – 8), the phosphate groups of ATP should be fully deprotonated.[17] Accordingly, the His122 residue is likely to be positively charged to optimize its electrostatic interaction with the negatively charged phosphate group of ATP. This would also avoid the assumption of an exceptionally low pK_a for the His122 residue, an argument that was used to explain the small variation of k_{cat}/K_m between pH values 6 – 9.[7] In a similar manner to results obtained for UMP/CMP kinase,[20] we found that the His122 residue should be doubly protonated in the presence of ATP, while it is neutral in the complex with ADP and AlF_3. Our assignment of these protonation states is mainly based on our results from geometric optimizations of the corresponding model system with ADP and AlF_3, which is in good agreement with X-ray data, especially with regard to the Al—N_δ and Al—O distances.

Optimization of the ATP complex with a neutral His122 residue did not give stable structures for reactant and product states whereas convincing geometries were obtained with a protonated His122 residue. Secondly, our product (His122—PO_3H · ADP) is 66.9 kJ mol^{-1} higher in energy than the reactants (His122—H · ATP) while the supposed product that contains unprotonated histidine (His122—PO_3 · ADP) is destabilized by 146.3 kJ mol^{-1} compared to the relaxed intermediate-like structure it adopts upon energy minimization. Conversely our reactant and product geometries are stable minima. Furthermore it is known that phosphohistidine is kinetically unstable and its energy of hydrolysis is more negative than that of ATP.[7] Both experimental findings support the existence of a high-energy phosphohistidine as represented by our product (His122—PO_3H · ADP). The protonation of the His122 residue in the presence of ATP by no means rules out the presence of unprotonated histidine in the free enzyme over a large pH range. The observed decrease in activity at pH values above 9 could therefore result from the lack of protonation of the His122 residue rather than the previously suggested deprotonation of Lys16 and Tyr56 residues.[7]

The observed reaction mechanism of phosphoryl transfer involves the synchronous shift of a proton from the N_δ atom of the His122 residue to the O1C oxygen atom of the γ PO_3 group as this group is transfered. This mechanism was found for all the substrates investigated. Such a proton shift is not commonly taken into account in the discussion of the reaction mechanism of kinases. To decide whether the reaction mechanism has more associative or dissociative character, the distance criteria in the transition state can be used. For the reaction with ATP the distances between the P_γ atom and its apical ligands suggest a dissociative type of mechanism as the sum of both distances (4.216 Å) is larger than the sum of two single covalent P—O bonds (around 3.4 Å).[1] We found a similar value (4.083 Å) in our previous study on UMP/CMP kinases, where a proton shift was also observed.[20] In the reactant and the transition state of the phosphoryl transfer in NDPK, the hydrogen atom of the ribose 3′-OH group forms a hydrogen bond to the O3C oxygen atom of the γ phosphate group and thus facilitates the phosphoryl transfer step. Except in the case of AMP-PNP, we did not observe a proton shift from the 3′-OH group to the γ phosphate group, presumably because the negative charge on the transferred PO_3 group is compensated by the simultaneous shift of the proton from the His122 atom to the O1C oxygen atom. This mechanism therefore complies with the phosphoryl transfer mechanism in UMP/CMP kinase and in cAPK as previously outlined by computational studies.[20–22]

Interpretations of our calculated reaction barriers have to consider the intrinsic error of semiempirical molecular orbital calculations.[25] More accurate calculations that use, for example, density functional theory, will help refine the computed barriers in future. Nevertheless, the structural and energetic results are comparable to or more accurate than computationally more expensive molecular orbital methods, such as ab initio, Hartree – Fock, and density functional methods. This accuracy means that the computed reaction mechanisms are essentially the same as would result from these other methods.[26]

Although the error involved can be be larger for transition states than for stable minima, the relative energy differences reflect the different stabilities of similar molecular systems. This allows a qualitative ranking of the NDPK substrates investigated in conjunction with the experimental data available.[4–6] Surprisingly, all of the computed reaction barriers for the (reversible) phosphoryl transfer lie within a narrow range of less than 23.0 kJ mol^{-1}, where AZT-TP and the hypothetical 2′-hydroxy-TTP

mark the upper and lower limits. Of the native triphosphate nucleosides, phosphoryl transfer to the His122 residue is best carried out by ATP, as expected. The reaction barriers for phosphorylation of the diphosphate nucleosides ADP, GDP, 2′-dATP, dTDP, D4T-DP, and AZT-DP are calculated to be within 4.4 kJ mol^{-1} of each other. Among the naturally occurring nucleosides the highest barrier is calculated for the phosphorylation of ADP (81.5 kJ mol^{-1}) which, however, would regenerate the ATP that is used to phosphorylate NDPK beforehand. Thus our calculations indicate that this unwanted reverse reaction is presumably avoided in biosynthesis by a high reaction barrier. An exception among the series of investigated nucleosides is AMP-PNP, which shows the highest reaction barrier but yields a different product. As AMP-PNP is a competitive inhibitor of other kinases it also marks an upper limit for the activation barrier in NDPK.

Substitutions of the OH group in the 2′- or 3′-position of the ribose moiety are associated with increased reaction barriers for the forward reaction ($\Delta H^{\neq}$(XTP $\rightarrow$ E $\sim$ P); X = any nucleoside), and lead to destabilization of the corresponding systems that contain the diphosphate (E $\sim$ P:MgXDP) as can be seen from the reaction enthalpies (see Figure 1 and Table 1). The destabilization of the diphosphate complex in turn influences the reaction barrier for the backward reaction ($\Delta H^{\neq}$(E $\sim$ P $\rightarrow$ XTP)), which yields the triphosphate nucleoside. Therefore no consistency of the latter reaction energy barriers is found upon substitution.

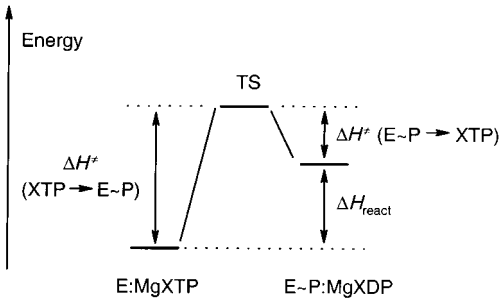

Figure 1. *Energy profile of the catalytic phosphoryl transfer from a triphosphate (XTP) to the enzyme (E) and backwards from the phosphorylated enzyme (E $\sim$ P) to a diphosphate (XDP) with the corresponding reaction barriers $\Delta H^{\neq}$. The computed energies for the investigated nucleoside systems are given in Table 1.*

Among the investigated dinucleoside systems, E $\sim$ P:MgADP is calculated to be the most stable (see third column in Table 1), except for the system that contains TDP, which is not naturally occurring. Nucleoside systems that have the 2′-OH group replaced by hydrogen, that is 2′-dATP and dTTP, are higher in energy than the ATP and TTP systems by 6.7 and 5.3 kJ mol^{-1}, respectively. When the 3′-OH group is removed (3′-dADP, D4T-DP, and AZT-DP), the destabilization is more drastic (13.1 – 16.5 kJ mol^{-1}), which underlines the favorable interaction of this hydroxy group with the γ phosphate group. These energy differences do not arise from differences in binding enthalpies since removal of individual hydrogen bond donors on the ligand may change the binding affinity only marginally, as shown previously for complexes of cAMP-dependent protein kinase and balanol derivatives.[27] Moreover, a significant amount of enthalpy – entropy compensation was reported for binding among this class of nucleosides.[5]

Comprehensive statements regarding the energetic differences in the stabilities of the enzyme – substrate complexes, for example, exact quantification of the binding energy of AZT-DP versus ADP, would require the computation of free energy perturbation profiles[28] for all NDPK – ligand systems and a proper treatment of solvation effects for the unbound ligands, which is beyond the scope of this work. However, as the various substrates investigated here do not significantly differ in their molecular shape and number of rotatable σ bonds, most of the entropic changes may be negligible. Nevertheless, we make no predictions concerning binding enthalpies but rather focus on the influence of the substrates on the relative stability of the complexes that contain the various phosphorylated enzymes (E $\sim$ P:MgXDP) compared to the corresponding system that contains the triphosphate (E:MgXTP). The associated energy differences (ΔH_{react}, see Table 1) thus reflect the substrate properties of the bound nucleoside diphosphates and agree well with experimental binding affinity data, for example, dTDP is a better substrate than AZT-DP.[4, 29]

The equilibrium constant K_{eq} for the equilibrium shown in Equation (3) is on the order of 1.[30]

$$\text{NDPK} + \text{ATP} \leftrightarrow \text{NDPK} \sim \text{P} + \text{ADP} \quad (3)$$

The binding constant of ATP with a H122G mutant of NDPK was measured as 0.2 μM ($\Delta G_{bind} = -38.9$ kJ mol^{-1})[4] and that of ADP with H122G and wild-type NDPK as 25 μM ($\Delta G_{bind} = -24.2$ kJ mol^{-1}) in both cases.[4] We expect the binding free energy of ADP to phosphorylated NDPK to be slightly less favorable than the number given as a result of the unfavorable electrostatic interaction of the negatively charged His122 $\sim$ P moiety with ADP. From these numbers, when possible conformational transitions of the protein and ligands are ignored, one would expect an endothermic reaction free energy of roughly 15 kJ mol^{-1} for the phosphoryl transfer from ATP to the His122 residue considered in this study. The computed value of 66.9 kJ mol^{-1} together with the energy barrier of 148.4 kJ mol^{-1} seems therefore a bit high. It remains to be seen whether these values are lower when found by using more accurate density functional calculations. The small variation found between ATP and nucleoside analogues, which is the important conclusion of this work, is unaffected by this possible shortcoming.

Conclusions

The catalytic reaction mechanism of phosphoryl transfer from triphosphate nucleosides to the His122 residue of NDPK and from the phosphorylated enzyme to diphosphate nucleosides was investigated by using semiempirical molecular orbital calculations on an active-site model of NDPK. On the basis of

the computational results it is suggested that the His122 residue is doubly protonated in the presence of bound triphosphates and unprotonated in the complex that contains ADP and AlF_3, in agreement with X-ray crystallographic data.

Phosphorylation of the enzyme is associated with a synchronous shift of the N_δ proton from a histidine residue to that oxygen atom of the γ phosphate group which is coordinated to the magnesium ion. As a result of the presence of the shifted proton, the transition state is not a planar PO_3 group; this geometry occurs further along the reaction path and leads to inversion of the configuration at the P_γ atom. This mechanism was found for all the triphosphates investigated and is analogous to the phosphoryl transfer mechanism suggested previously for cAPK and for UMP/CMP kinase.

NDPK is able to process the ATP analogue AMP-PNP, which is a competitive inhibitor of other kinases.[7] This is a result of the specific binding pocket of NDPK that allows interaction with the 3′-OH group of the ribose moiety. In the case of AMP-PNP only, active participation of this hydroxy-group hydrogen atom leads to proton abstraction by the intermediate imido anion, which forms an energetically more favorable hydroxylate anion. For all other nucleosides no such shift of this proton to either the β or γ phosphate group was observed. According to the proposed mechanism, which involves proton abstraction from the 3′-OH group, NDPK should not be able to process 5′-[β,γ-imido]-3′-deoxyribose adenosine triphosphate. This reasoning provides an opportunity for experimental verification of the mechanism.

The presence of the N_3 group in AZT was found to be sterically and electrostatically unfavorable and causes structural rearrangement of the side chain of the Asn119 residue in our model. This explains some of the poor substrate properties of AZT, especially when compared to D4T-DP, which is well accommodated into the active site and shows favorable electrostatic interactions and steric behaviour.

The computed activation enthalpies for the phosphorylation of the diphosphates by the enzyme ($E\sim P \rightarrow XTP$) are within 13.1 kJ mol^{-1} for all substrates. This value includes the nucleosides that do not possess a 3′-OH group, such as AZT-DP and D4T-TP. These reaction barriers do not substantially differ between good and poor substrates as the barrier is also dependent on the destabilization of the diphosphate system compared to the corresponding triphosphate. The amount of destabilization gives, however, a qualitative ranking of the substrate properties since its range of about 17 kJ mol^{-1} agrees with known experimental binding affinities, which vary over a similar range (13 kJ mol^{-1}).[5]

These data together suggest that the individual binding properties of the diphosphate nucleosides and the height of the reaction barrier control the enzymatic turnover in NDPK to a similar extent. This is of particular interest for the development of new anti-HIV nucleoside analogues, as their design should therefore be optimized first for high binding affinities. On the basis of our computational findings, the most promising drug candidates are thus 3′-deoxynucleosides in which the substituents of the ribose moiety can form electrostatically favorable interactions with the oxygen atoms of the γ phosphate group.

Methods

For the computational investigation of NDPK a structural model system was set up for the active site (shown in Scheme 2) based on crystallographic data for Dd-NDPK. The active site is buried in the binding pocket for the nucleosides and thus effects of the exterior solvent on the reaction mechanism are not explicitly taken into account. The procedure for the generation of this model system is analogous to that used in previous studies.[20, 21] The model system contains ATP, the Mg^{2+} ion with three coordinating water molecules, and various residues thought to be critical for the phosphoryl transfer. These components make a total of 221 atoms all of which are given a full quantum mechanical treatment by the semiempirical AM1 method.[25] All calculations were performed on a modified version of the program package VAMP Version 6.5[31] The same parameter sets were employed for phosphorus[32] and magnesium[33] as in earlier studies on related kinases.[20, 21]

Initial atomic coordinates of the nonhydrogen atoms in the model system were taken from the chain A X-ray crystallographic structure of Dd-NDPK complexed with ADP and the transition state analogue AlF_3 (1KDN)[17]. The crystallographic water molecules at positions 671, 690, and 698 were included to complete the octahedral coordination sphere of the magnesium ion. Water molecules 612, 650, 721, 728, and 775 are also present because they are part of the hydrogen bond network between active-site residues in our model system.

AlF_3 was replaced by PO_3 to form the γ phosphate group of ATP. This is not expected to cause noticeable structural changes in the active site as crystal structures of various nucleosides show that variations in the region of the phosphoryl groups have no influence on the binding mode of the nucleotide moiety, nor on the overall protein structure.[9]

The residues in the vicinity of the reactants His122 and ATP that were considered included three arginine residues (92, 109, and 132), which were truncated at the C_δ atom. The Asp125 residue was capped at the C_β atom and likewise the Glu133 and Glu53 residues were capped at the C_γ atom. The Tyr56, Thr98, Asn119, and His122 residues were included with their complete side chains and the corresponding backbone atoms. The terminal C_δ–CH_2–NH_3 group of the Lys16 residue was included. In a similar approach to that of side-chains truncatation, only the carbonyl fragments of Ser54, His55, Val97, and Ile121, which are involved in hydrogen bonding, were modeled (see Scheme 2).

Hydrogen atoms were added with initial bond lengths of 1.08 Å, which assumes that the side chains of aspartate, glutamate, arginine, and lysine are charged. Together with the doubly protonated His122 residue (see below), this results in a net neutral charge for the model system.

To emulate the structural effect of the protein backbone, some of the nonhydrogen atoms of the truncated residues were harmonically restrained to their crystallographic positions. Compared to a fully rigid fixation this approach offers the advantage that stationary points on the energetic hypersurface (minima and transition states) can still be characterized.[34] Also, the "hardness" of each harmonic potential can be adjusted to suit the particular environment of each atom. Restraints in the order of 21 – 85 kJ mol^{-1} have been shown to be sufficient for combined quantum mechanical/molecular modeling calculations where the active site of the protein is represented by a quantum mechanical function surrounded by the remaining protein modeled by molecular mechanics.[35] In this study, however, no such surrounding environment is present and thus stronger restraints are necessary to emulate the absent protein backbone. For

all carbon atoms that terminate a side chain of aspartate, glutamate, arginine, or lysine a strong force constant of 4820 kJ mol^{-1} Å^{-2} was employed. For the backbone atoms involved in peptide bonds, the same force constant was applied to the carbon and nitrogen atoms, while a softer potential of 1927 kJ mol^{-1} Å^{-2} was used for the oxygen atoms. As the computational model cannot account for the steric effect of absent amino acids in the outer part of the protein, it was found necessary to restrain several carbon atoms in the side chains with a force of 4820 kJ mol^{-1} Å^{-2} as well, notably C_δ of glutamate, C_γ of aspartate, C_β of tyrosine, asparagine, and histidine, and C_α of threonine, while a softer potential proved to be sufficient for the C_ζ atom in Arg132. For the oxygen atoms of the three water molecules that ligate the magnesium ion, a very weak force constant of 0.084 kJ mol^{-1} Å^{-2} was employed to allow structural movement. Similarly, no constraints were applied to ATP. For the oxygen atoms of the remaining water molecules a potential of 966 kJ mol^{-1} Å^{-2} was used as these atoms were either found to be conserved among various X-ray structures or to terminate the active site model. Moreover, the crystallographic structures of the holoenzyme, the phosphohistidine, and the transition state analogue show only slight root mean square deviations, that is, no distinct movement of particular amino acids is expected during the phosphoryl transfer step. Altogether 38 out of the 221 atoms of the ATP-bound system were restrained in some way.

A step width of 0.05 Å was used in the reaction path calculations while a (strong) force constant of 48 1954 kJ mol^{-1} Å^{-2} was applied to move the P_γ atom towards the N_δ atom of the His122 residue. A potential with a parabolic shape along the reaction coordinate was used between the shifted proton and its target atom. This potential has its minimum at zero in the middle of the reaction path and rises to a maximum of 96391 kJ mol^{-1} Å^{-2} at the start and at the end of the reaction coordinate. Compared to conventional calculations where the shifted atoms are fully fixed in spatial positions along the given reaction coordinate, which corresponds to an infinitely high force constant, the potential used here allows a smoother sampling of a larger conformational space during the reaction path calculation while reactant and product geometries remain well determined. Transition states were identified by computation of their harmonic vibrational frequencies. At the transition state the matrix of the secondary derivatives shows one negative eigenvalue referred to as imaginary frequency (given in wave numbers in units of cm^{-1}). This value corresponds to the motion of the molecular system over this saddle point. The eigenvector following algorithm[36] was used throughout all calculations to optimize the molecular system to a gradient norm below 1.67 kJ mol^{-1} Å^{-1}.

Structural coordinates of the employed quantum mechanical system are provided in the Supporting Information in the form of Protein Databank files for the reactants, transition state, and products of the phosphoryl transfer that involves ATP.

We thank Dr. Jochen Reinstein and Dr. Friedrich Herberg for critical reading of the manuscript.

[1] A. S. Mildvan, *Proteins* **1997**, *29*, 401 – 416.
[2] D. Bossemeyer, *FEBS Lett.* **1995**, *369*, 57 – 61.
[3] A. de la Rosa, R. L. Williams, P. S. Steeg, *Bioessays* **1995**, *17*, 53 – 62.
[4] B. Schneider, R. Biondi, R. Sarfati, F. Agou, C. Guerreiro, D. Deville-Bonne, M. Véron, *Mol. Pharmacol.* **2000**, *57*, 948 – 953.
[5] L. Cervoni, I. Lascu, Y. Xu, P. Gonin, M. Morr, M. Merouani, J. Janin, A. Giartosio, *Biochemistry* **2001**, *40*, 4583 – 4589.
[6] J. Bourdais, R. Biondi, S. Sarfati, C. Guerreiro, I. Lascu, J. Janin, M. Véron, *J. Biol. Chem.* **1996**, *271*, 7887 – 7890.
[7] I. Lascu, P. Gonin, *J. Bioenerg. Biomembr.* **2000**, *32*, 237 – 246.
[8] A. D. Tepper, H. Dammann, A. A. Bominaar, M. Véron, *J. Biol. Chem.* **1994**, *269*, 32 175—32 180.
[9] J. Janin, C. Dumas, S. Moréra, Y. Xu, P. Meyer, M. Chiadmi, J. Cherfils, *J. Bioenerg. Biomembr.* **2000**, *32*, 215 – 225.
[10] Kreimeyer, Annett, B. Schneider, R. Sarfati, A. Faray, J.-P. Sommadossi, M. Véron, D. Deville-Bonne, *Antiviral Res.* **2001**, *50*, 147 – 156.
[11] P. Gonin, Y. Xu, L. Milon, D. Sandrine, M. Morr, R. Kumar, M.-L. Lacombe, J. Janin, I. Lascu, *Biochemistry* **1999**, *38*, 7265 – 7272.
[12] R. E. Parks Jr., R. P. Agarwal in *Group Transfer Part A, Vol. 8* (Ed.: P. D. Boyer), Academic Press, New York, **1973**, pp. 307 – 334.
[13] A. Lecroisey, I. Lascu, A. Bominaar, M. Veron, M. Delepierre, *Biochemistry* **1995**, *34*, 12 445 – 12 450.
[14] S. Moréra, M. Chiadmi, G. LeBras, I. Lascu, J. Janin, *Biochemistry* **1995**, *34*, 11062 – 11070.
[15] I. Lascu, R. D. Pop, H. Porumb, E. Presecan, I. Proinov, *Eur. J. Biochem.* **1983**, *135*, 497 – 503.
[16] S. Moréra, G. LeBras, I. Lascu, M.-L. Lacombe, M. Véron, J. Janin, *J. Mol. Biol.* **1994**, *243*, 873 – 890.
[17] Y.-W. Xu, S. Moréra, J. Janin, J. Cherfils, *Proc. Natl. Acad. Sci. USA* **1997**, *94*, 3579 – 3583.
[18] S. J. Admiraal, D. Herschlag, *Chem. Biol.* **1995**, *2*, 729 – 739.
[19] I. Schlichting, J. Reinstein, *Biochemistry* **1997**, *36*, 9290 – 9296.
[20] M. C. Hutter, V. Helms, *Protein Sci.* **2000**, *9*, 2225 – 2231.
[21] M. C. Hutter, V. Helms, *Protein Sci.* **1999**, *8*, 2728 – 2733.
[22] J. C. Hart, D. W. Sheppard, I. H. Hillier, N. A. Burton, *Chem. Commun.* **1999**, 79 – 80.
[23] Y.-W. Xu, O. Sellam, S. Moréra, S. Sarfati, R. Biondi, M. Veron, J. Janin, *Proc. Natl. Acad. Sci. USA* **1997**, *94*, 7162 – 7165.
[24] P. Meyer, B. Schneider, S. Sarfati, D. Deville-Bonne, C. Guerreiro, J. Boretto, J. Janin, M. Véron, B. Canard, *EMBO J.* **2000**, *19*, 3520 – 3529.
[25] M. J. S. Dewar, E. G. Zoebisch, E. F. Healy, J. J. P. Stewart, *J. Am. Chem. Soc.* **1985**, *107*, 3902 – 3909.
[26] M. J. Field, *J. Comput. Chem.* **2002**, *23*, 48 – 58.
[27] P. Hünenberger, V. Helms, N. Narayana, S. S. Taylor, J. A. McCammon, *Biochemistry* **1999**, *38*, 2358 – 2366.
[28] P. A. Kollman, *Chem. Rev.* **1993**, *93*, 2395 – 2417.
[29] B. Schneider, Y. W. Xu, O. Sekkan, R. Sarfati, J. Janin, M. Véron, D. Deville-Bonne, *J. Biol. Chem.* **1998**, *273*, 11 491—11 497.
[30] M. Brune, J. E. T. Corrie, M. R. Webb, *Biochemistry* **2001**, *40*, 5087 – 5094.
[31] G. Rauhut, A. Alex, J. Chandrasekhar, T. Steinke, W. Sauer, B. Beck, M. Hutter, P. Gedeck, T. Clark, VAMP Version 6.5, Oxford Molecular, Erlangen, **1997**.
[32] M. J. S. Dewar, C. X. Jie, *THEOCHEM* **1989**, *187*, 1 – 13.
[33] M. C. Hutter, J. R. Reimers, N. S. Hush, *J. Phys. Chem. B* **1998**, *102*, 8080 – 8090.
[34] T. Clark, P. Gedeck, H. Lanig, G. Schürer in *Molecular Modelling and Dynamics of Bioinorganic Systems, Vol. 41* (Eds.: L. Banci, P. Comba), Kluwer Academic Publishers, Dordrecht, **1997**, pp. 307 – 318.
[35] G. Schürer, H. Lanig, T. Clark, *J. Phys. Chem. B* **2000**, *104*, 1349 – 1361.
[36] J. Baker, *J. Comput. Chem.* **1986**, *7*, 385 – 395.

Received: February 8, 2002 [F 360]